

The rise and fall of F_2 at low x

A M COOPER-SARKAR & R.C.E DEVENISH

Department of Physics, University of Oxford, Denys Wilkinson Bldg, Keble Rd,
Oxford OX1 3RH, UK

A short personal account is given of the impact of HERA data and the influence of Jan Kwiecinski on low x physics.

1. Introduction

That HERA data was to change our understanding of pQCD was announced at the Durham Phenomenology Workshop on HERA Physics in 1993 (the first of three devoted to HERA Physics, all with a large input from JK). Albert De Roeck presented the first preliminary H1 data from HERA on F_2 measurements at $x < 0.01$, below the fixed target region. Within large errors that data showed a rising F_2 as x decreased – the quality of the data may be judged from Fig 1 showing comparable ZEUS data. The result was the major talking point of the 1993 HERA workshop and discussion has continued almost unabated since then. One gets a sense of why the result was surprising by comparing Fig 1 with Fig 2. The latter plot shows a range of predictions from a paper by Askew, Martin, Kwiecinski & Sutton (AKMS) [2] with F_2 data from the NMC and BCDMS experiments for $x > 0.01$. The least model-dependent extrapolation from the measured data would appear give a ‘flat’ F_2 as $x \rightarrow 0$ as shown by the dash-dotted curve, but what do the rising curves represent?

2. F_2 in pQCD

A rising F_2 at small- x is predicted by pQCD, but the predictions do not give a scale in either x or Q^2 at which one might expect to see such effects. In the DGLAP¹ formalism at leading order the gluon splitting functions

$$P_{gq} \rightarrow \frac{4}{3z}, \quad P_{gg} \rightarrow \frac{6}{z} \quad (1)$$

¹ Dokshitzer, Gribov, Lipatov, Altarelli & Parisi, collinear factorization.

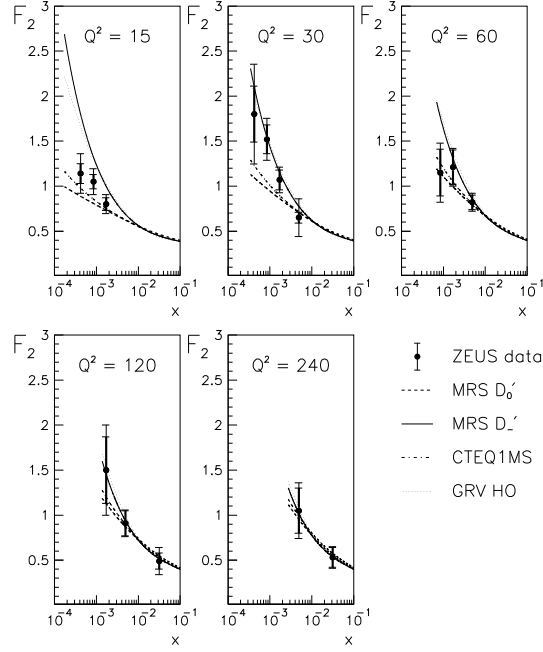


Fig. 1. The first ZEUS F_2 data from HERA, published 1993 [1].

are singular as $z \rightarrow 0$. Thus the gluon distribution will become large as $x \rightarrow 0$, and its contribution to the evolution of the parton distribution becomes dominant. In particular the gluon will ‘drive’ the quark singlet distribution, and hence the structure function F_2 , to become large as well, the rise increasing in steepness as Q^2 increases. Quantitatively,

$$\frac{dg(x, Q^2)}{d \ln Q^2} \simeq \frac{\alpha_s(Q^2)}{2\pi} \int_x^1 \frac{dy}{y} \frac{6}{z} g(y, Q^2) \quad (2)$$

may be solved subject to the nature of the boundary function $xg(x, Q_0^2)$. Inputting a non-singular gluon at Q_0^2 , the solution is [4, 5]

$$xg(x, Q^2) \simeq \exp \left(2 \left[\xi(Q_0^2, Q^2) \ln \frac{1}{x} \right]^{\frac{1}{2}} \right) \quad (3)$$

where

$$\xi(Q_0^2, Q^2) = \int_{Q_0^2}^{Q^2} \frac{dq^2}{q^2} \frac{3\alpha_s(Q^2)}{\pi} \quad (4)$$

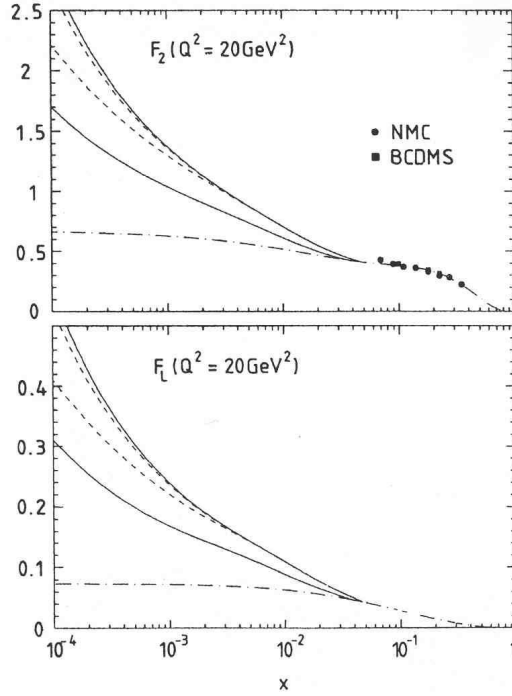


Fig. 2. Calculations from AKMS [2] of the behaviour of F_2 and F_L at low x based on the BFKL equation. The difference between the upper and lower continuous curves is in the cut-off imposed to control diffusion in transverse momentum ($k_0^2 = 1, 2 \text{ GeV}^2$ for the upper, lower curves respectively). The dashed curves show the effect of including shadowing effects with a proton radius of $R = 5, 2 \text{ GeV}^{-1}$. The almost flat dash-dotted curves are the contributions excluding the BFKL effects.

Given a long enough evolution length from Q_0^2 to Q^2 , this will generate a steeply rising gluon distribution at small x , starting from a flattish behaviour of $xg(x, Q^2)$ at $Q^2 = Q_0^2$.

Over the x, Q^2 range of HERA data this solution mimics a power behaviour, $xg(x, Q^2) \sim x^{-\lambda_g}$, with

$$\lambda_g = \left(\frac{12 \ln(t/t_0)}{\beta_0 \ln(1/x)} \right)^{\frac{1}{2}} \quad (5)$$

where $t = \ln(Q^2/\Lambda^2)$, $t_0 = \ln(Q_0^2/\Lambda^2)$. This steep behaviour of the gluon generates a similarly steep behaviour of F_2 at small x , $F_2 \sim x^{-\lambda}$, where $\lambda = \lambda_g - \epsilon$.

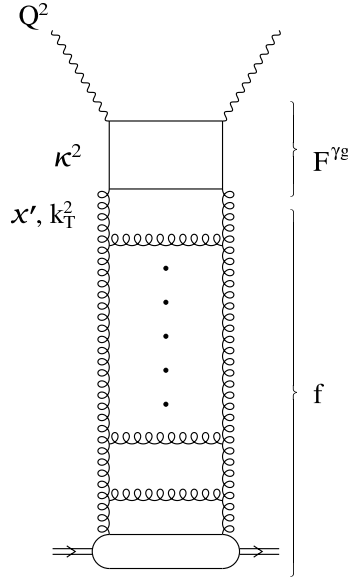


Fig. 3. The BFKL gluon ladder diagram for deep inelastic scattering with a quark box at the top connecting to the γ^* and the proton at the bottom.

So why was the observed rise of F_2 unexpected? Because, before the advent of HERA data, the starting scale for perturbative evolution had always been taken to be $Q_0^2 \gtrsim 4 \text{ GeV}^2$, to be sure that a perturbative calculation would be valid. The evolution length from Q^2 of 4 to 15 GeV^2 is not large enough to generate a steep slope from a flat input.

However Jan Kwiecinski together with Martin, Roberts and Stirling [3] had already been considering alternatives to ‘conventional’ DGLAP with flat input distribution. The KMRSB_0 and KMRSB_- parton distribution functions of 1990 [3] were both compatible with the data: KMRSB_0 had a conventional flat gluon distribution input at $Q_0^2 = 4 \text{ GeV}^2$; whereas KMRSB_- had a singular gluon distribution $x^{-0.5}$, even at low $Q^2 (= Q_0^2)$.

Why should one consider a steep input gluon?. Because at small x terms in $\ln(1/x)$ are becoming large and the conventional *leading* $\ln Q^2$ summation of the DGLAP equations does not account for this. It may also be necessary to sum *leading* $\ln(1/x)$ terms. Such a summation is performed by the BFKL² equation. To leading order in $\ln(1/x)$ with fixed α_s , this predicts a steep power law behaviour

$$xg(x, Q^2) \sim f(Q^2) x^{-\lambda_g} \quad (6)$$

² Balitsky, Fadin, Kuraev & Lipatov, k_T factorization.

where

$$\lambda_g = \frac{3\alpha_s}{\pi} 4 \ln 2 \simeq 0.5 \quad (7)$$

(for $\alpha_s \simeq 0.2$, as appropriate for $Q^2 \sim 4 \text{ GeV}^2$).

These ideas were taken further in the paper by AKMS, see Fig. 2, in which BFKL evolution was incorporated directly into the calculation of the parton densities. The rising curves show different calculations of F_2 and F_L from the BFKL equation, the dashed curves show the effect of including some damping by shadowing which will be discussed later. The dash-dotted curve is the prediction for the structure functions without BFKL effects.

Thus the observation of a steep behaviour in F_2 at a relatively low Q^2 was seized upon by those who saw this as evidence for BFKL. On the other hand it was quickly realised that by lowering the starting scale in the DGLAP approach to $Q_0^2 \approx 1 \text{ GeV}^2$ one could also fit the data without a singular gluon input distribution. This later approach owed much to the work of Glück, Reya and Vogt (GRV) [6]. Higher statistics data taken during 1993 showed that an effective power $\lambda_g \approx 0.5$ was actually too steep.

Kwiecinski was involved with many of the approaches to find a credible phenomenology of the BFKL equation. One of the most significant of these is the need for a ‘kinematic constraint’ to control the diffusion of transverse momentum down the ‘gluon ladder’ in the BFKL approach (see Fig. 3). Unlike the DGLAP summation in which the k_T of the ladder are strictly ordered, those in the BFKL summation are not and can diffuse downwards into the non-perturbative region. Consider a link in the gluon chain where the longitudinal momentum fraction decreases from x/z to x and the transverse momentum k'_T changes to k_T , with emission of a gluon of transverse momentum q_T . One requires

$$k_T^2/z > q_T^2 \quad (8)$$

in order that the virtuality of exchanged gluons is controlled by their transverse momenta. This implies that $k_T^2/z > k_T'^2$, for any given value of k_T . If one considers the effect of this constraint on the solutions for the BFKL equation one finds that it modifies the asymptotic solution $x^{-\lambda_g}$, such that λ_g is reduced from $\lambda_g \sim 0.5$ to $\lambda_g \sim 0.3$. These ideas were built into an ambitious approach by Kwiecinski, Martin and Stasto [8] to combine the BFKL and DGLAP approaches in a single model to be applied to the HERA and fixed target data. The key idea was to use the BFKL kernel, with the kinematic constraint, applied to the unintegrated gluon density (i.e. differential in k_T as well as x) to give an input gluon density to DGLAP evolution. This gives rise to a pair of coupled equations for the gluon and $q\bar{q}$ sea which can be solved numerically. The small valence quark contribution was taken from the leading order GRV set [9] to give a complete model for F_2 , F_2^{charm} and

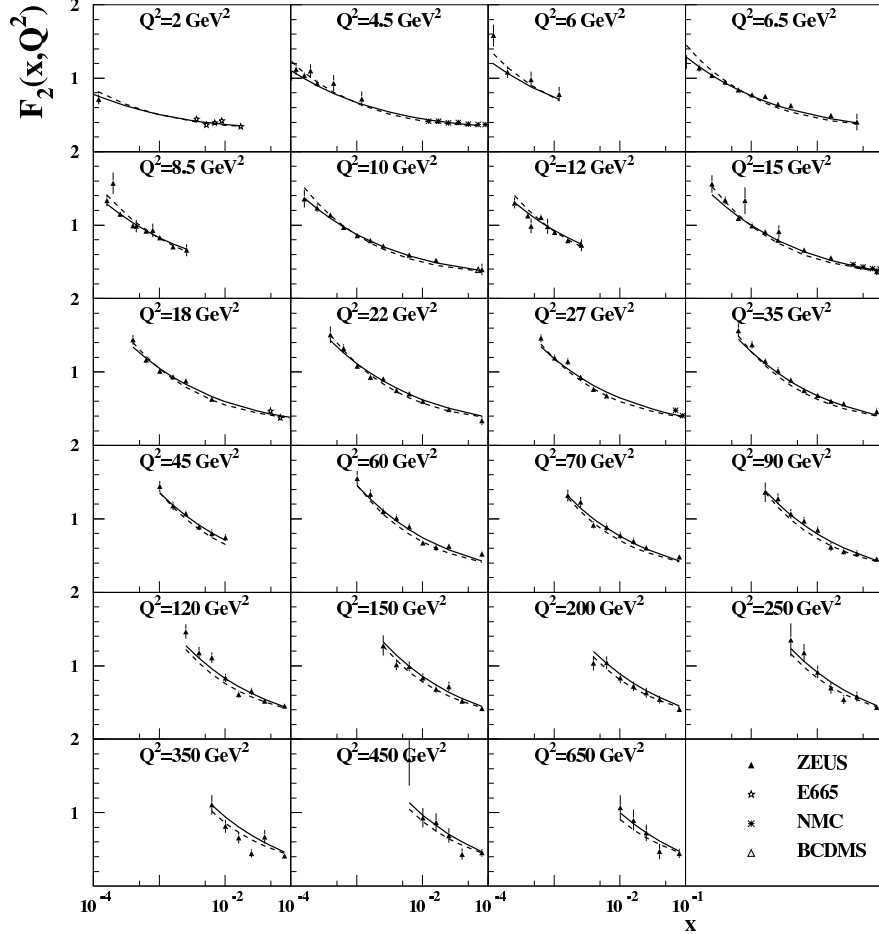


Fig. 4. The combined BFKL-DGLAP model of KMS fit to F_2 data from ZEUS, E665, BCDMS & NMC. From [8].

F_L . Only two parameters were needed to describe $xg(x, k_0^2)$ at the starting scale. A very good fit to the HERA 1994 F_2 data together with data from E665, BCDMS and NMC was obtained, as shown in Fig. 4.

During the period 1994 – 1996 the conventional DGLAP NLO QCD global fits were also refined and gave very good χ^2 fits to the HERA data, starting with a conventional flat gluon input, provided that a low starting scale $Q_0^2 = 1 \text{ GeV}^2$ was used. In 1996 the HERA data from the 1994 run were published, showing that that the steep slope of F_2 extended as far down in Q^2 as $Q^2 \sim 1.5 \text{ GeV}^2$. The precision of the data had now increased

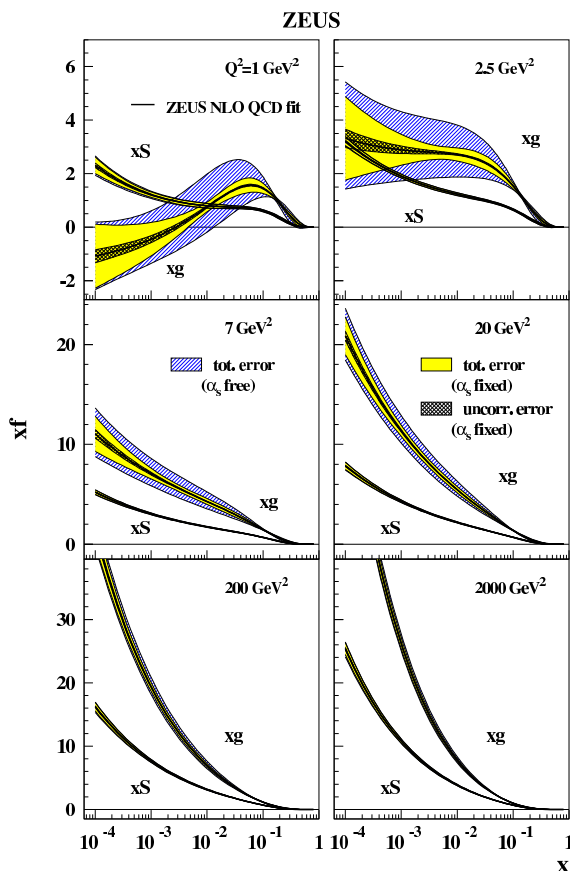


Fig. 5. Gluon and sea quark momentum distributions compared. From a NLO QCD fit by ZEUS using the full HERA-I data sample [7].

sufficiently that the low- x behaviour of the sea and the gluon distributions could be fitted separately. These results led to a new kind of surprise since it became clear that the flat input which had been used for both the sea and the gluon ($\lambda_S = \lambda_g \sim 0$) was actually a compromise between a sea distribution which remains steep, $\lambda_S \sim 0.2$ down to $Q^2 \sim 1 \text{ GeV}^2$, and a gluon distribution which is becoming valence-like, $\lambda_g < 0$ at low Q^2 . Fig. 5 shows a recent result from a ZEUS global fit using the complete HERA-I data sample [7]. This behaviour contradicts the original argument that the steep behaviour of the gluon distribution is driving the steep behaviour of the sea which is measured in F_2 .

These conclusion were strengthened when the data from the 1996/7 runs

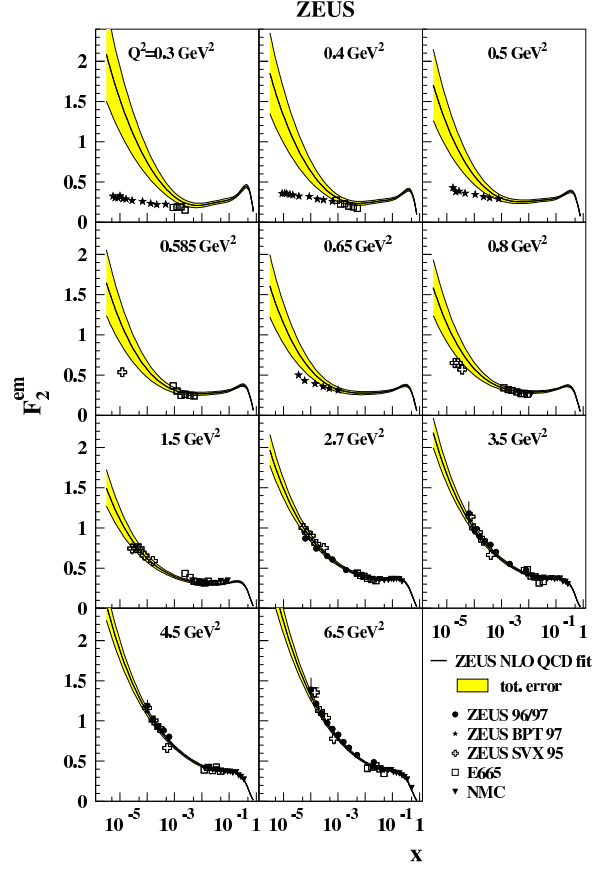


Fig. 6. ZEUS F_2 data at low Q^2 compared to the ZEUS-S pQCD fit [7].

were published in 2000/2001. It became possible to make detailed analyses of the experimental uncertainties on the parton distributions and thus put limits on the kinematic range of applicability of the DGLAP formalism. For $Q^2 \lesssim 1 \text{ GeV}^2$ the gluon distribution becomes negative at small x , see Fig. 5 and the fit can no longer describe the data, see Fig. 6. Furthermore, even though the DGLAP formalism works for $Q^2 \gtrsim 1 \text{ GeV}^2$, doubts remain about its applicability when $\lambda_g < \lambda_S$. With only one observable measured with high precision and all models depending on parameters fit to data, one has sufficient flexibility to get good descriptions in both the pure DGLAP and ‘BFKL enhanced’ approaches. The striking rise in F_2 does begin to abate for Q^2 below 2 GeV^2 as Fig. 6 illustrates. At this point is useful to bring in data on the slopes or derivatives of F_2 .

shown in Fig. 7. This is another result from HERA that caused a lot of interest and discussion! The plot shows the slopes calculated from the F_2 shown in Fig. 4. An important detail to note is that because of the strong correlation between x and Q^2 inherent in deep inelastic kinematics, the slopes are not evaluated at a fixed values of Q^2 , but rather at the mean values shown along the top of the plot for each data point. The plot shows that the rate of rise of F_2 as a function of Q^2 is starting to abate as $x < 10^{-3}$ and $Q^2 < 8 \text{ GeV}^2$. To understand what the plot might indicate and why one is also very interested in where and how F_2 stops rising at low x it is helpful to look at the HERA data from another point of view.

4. $\sigma(\gamma^*p)$ and saturation

The strong rise of F_2 at low x was unexpected for another reason. At small x , F_2 is related to the cross-section for γ^*p scattering by

$$\sigma^{\gamma^*p}(W^2, Q^2) \approx \frac{4\pi^2\alpha}{Q^2} F_2(x, Q^2), \quad \text{with } W^2 \approx Q^2/x, \quad (9)$$

where W is the γ^*p centre of mass energy. This relation implies that a rise of F_2 at small- x corresponds to a rising γ^*p cross-section with W^2 . The relationship above suggests another approach to understanding the behaviour of F_2 at low x and that is the framework of Regge theory used to explain the high energy behaviour of hadronic total cross-sections. Regge theory predicts that the high energy behaviour of hadronic scattering amplitudes is $\text{Im}A(ab \rightarrow cd) \sim \sum_i \beta_i s^{\alpha_i}$, where α_i is the intercept of a Regge trajectory which has the right quantum numbers for an exchange in the crossed channel $a\bar{c} \rightarrow \bar{b}d$. Using the optical theorem, a total cross-section will vary as $\sigma^{\text{tot}}(ab) \sim \sum_i \beta_i s^{\alpha_i - 1}$. For the corresponding forward elastic scattering amplitude, the leading Regge trajectory has the quantum numbers of the vacuum and is known as the Pomeron, for which the value $\alpha_P \approx 1.08$ has been determined from hadron-hadron data. This prediction also describes the high energy behaviour of photoproduction cross-section measurements successfully. The model was extended to describe virtual-photon proton scattering by Donnachie and Landshoff [11] who assumed that the Q^2 dependence would reside in the residue functions $\beta_i(Q^2)$ only and that the intercepts, α_i would be independent of Q^2 . Through Eq. 9 this approach then predicts a flattish input for the gluon and sea PDFs, since $\sigma(\gamma^*p) \sim s^{\alpha_i - 1}$ implies $F_2 \sim x^{1 - \alpha_i} = x^{-0.08}$. While the DL approach successfully described the pre-HERA low x data for Q^2 values up to about 10 GeV^2 , it cannot describe the steeply rising F_2 data measured

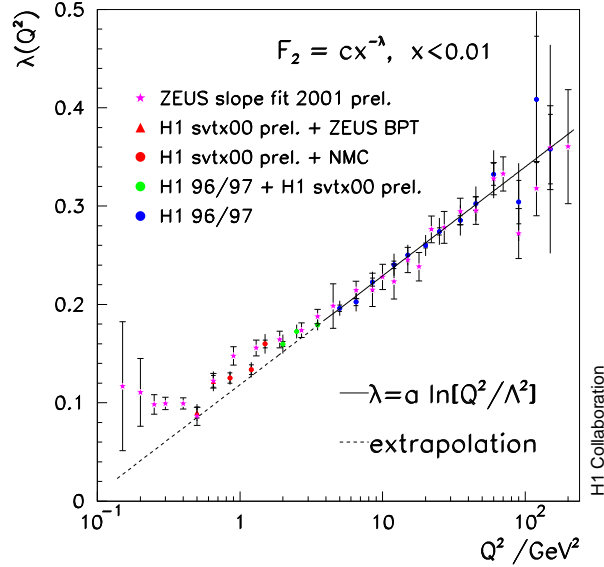


Fig. 8. The effective slope of F_2 at low x , $F_2 \sim x^{-\lambda(Q^2)}$. From [13].

at HERA. The problem is summarised graphically in Fig. 8 which shows $\lambda(Q^2) = \frac{\partial \ln F_2}{\partial \ln(1/x)}$ or $F_2 \sim x^{-\lambda(Q^2)}$, at low x . For Q^2 values less than 1 GeV^2 or so, the value of λ is consistent with that from hadronic Regge theory, whereas for $Q^2 > 1 \text{ GeV}^2$ the slope rises steadily to reach a value greater than 0.3 by $Q^2 \approx 100 \text{ GeV}^2$. This larger value of λ is not so far from that expected using BFKL ideas. Indeed the BFKL equation can be viewed as a method for calculating the hard or perturbative Pomeron trajectory – in contrast to the soft or non-perturbative Pomeron of hadronic physics with intercept around 1.08. Donnachie and Landshoff [12] have extended their Regge model by the addition of a hard Pomeron with intercept 1.44, which allows them to describe the low x HERA data up to Q^2 values of a few hundred GeV^2 . Theirs is one of many attempts, using ideas from Regge theory, to model the ‘transition region’ from real photoproduction through to deep inelastic scattering with $Q^2 \gg 1 \text{ GeV}^2$.

Either considering the rise of F_2 as $x \rightarrow 0$ or the steep energy dependence of $\sigma(\gamma^*p)$ at large Q^2 , such behaviour will eventually violate the Froissart bound. If the origin of the rise arises from a high gluon density then this problem may be avoided because the gluons can shadow each other from the γ^* . At even higher densities the gluons will ‘recombine’ via the process $gg \rightarrow g$ – the inverse of gluon splitting – and the gluon density and hence F_2

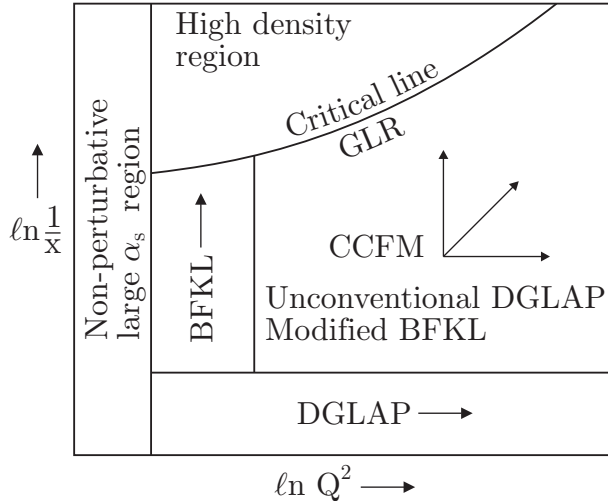


Fig. 9. Approaches to physics at low- x . Courtesy of A D Martin

will saturate. These ideas have been formalized by Gribov, Levin & Ryskin by the addition of a non-linear term to the equation for gluon evolution

$$\frac{d^2 xg(x, Q^2)}{d \ln Q^2 d \ln(1/x)} = \frac{3\alpha_s}{\pi} xg(x, Q^2) - \frac{81\alpha_s^2}{16Q^2 R^2} [xg(x, Q^2)]^2 \quad (10)$$

When $xg(x, Q^2) \sim \pi Q^2 R^2 / \alpha_s(Q^2)$ the non-linear term cancels the linear term and evolution stops, this is saturation. Shadowing effects were included in the calculations by AKMS shown in Fig. 2 and in the KMRS parton densities.

The various evolution equations applicable across the x, Q^2 plane are summarised schematically in Fig. 9.⁴ Note the appearance of the ‘critical line’ above which the gluon density is high enough for non-linear effects to be important. In this region and for large enough Q^2 one has the possibility that α_s will be small enough for weak-coupling but non-perturbative methods to be applicable, of which the GLR equation could be a first approximation. Again no scales are given and another of many hotly argued questions raised by the HERA data – for example in the context of the Caldwell plot (Fig. 7) – is does HERA have the reach to see saturation effects and have they been seen?

Dipole models have proved to be a very fruitful approach in exploring this question and modelling the behaviour of F_2 or $\sigma(\gamma^*p)$ through the

⁴ An early version of this figure was shown by JK in his plenary talk on low x QCD at the 1993 Durham Workshop [14].

transition region towards $Q^2 = 0$. The idea is that the virtual photon splits into a $q\bar{q}$ pair⁵ (a colour dipole) with a transverse size $r \sim 1/Q$, the splitting occurring a ‘long’ time $\sim 1/(mx)$ before the dipole interacts with the proton. The dipole then scatters coherently from the proton in a time which is short in comparison to $\sim 1/(mx)$. The $\gamma^* \rightarrow q\bar{q}$ process is described by QED and the strong interaction physics is then contained in the cross-section, $\hat{\sigma}$, for the dipole-proton interaction.

Many authors have worked on these models in the context of DIS processes both inclusive and for diffraction. Here the discussion will focus on the model of Golec-Biernat and Wüsthoff (GBW) [15]. The original GBW model provides a simple parameterization of $\hat{\sigma}$ with explicit saturation, in the sense that $\hat{\sigma} \rightarrow \sigma_0$ (a constant) as r becomes large, but in a such a way that the approach to saturation is x dependent, controlled by the ‘saturation radius’, R_0 . Explicitly the dipole cross-section is given by

$$\hat{\sigma}(x, r^2) = \sigma_0(1 - \exp(-\hat{r}^2)), \quad \hat{r} = \frac{r}{2R_0(x)} \quad (11)$$

where σ_0 is a constant, and

$$R_0(x)^2 = \frac{1}{Q_0} \left(\frac{x}{x_0} \right)^\lambda, \quad (12)$$

$R_0(x)^2$ is understood to be inversely proportional to the gluon density ($\lambda \sim \lambda_g$), so that R_0 is a measure of the transverse separation of the gluons in the target. Thus when the dipole separation is large compared to the gluon separation (small Q^2 and small x) the dipole cross-section saturates, $\hat{\sigma} \sim \sigma_0$, and $\sigma(\gamma^*p)$ also tends to a constant, giving $F_2 \propto 1/Q^2$ from Eq. 9. When the dipole separation is small compared to the gluon separation (high Q^2 and large x), $\hat{\sigma} \sim \sigma_0/(Q^2 R_0^2)$ and $\sigma(\gamma^*p)$ varies as $1/Q^2$, so that F_2 exhibits Bjorken scaling. Because of the x dependence of R_0 , $\hat{\sigma}$ saturates for smaller dipole sizes as x decreases.

Looking at Fig. 10, which shows F_2 as a function of Q^2 at fixed $y = Q^2/sx$, one sees that the data do exhibit these features. There is a clear change in behaviour around $Q^2 \approx 1 \text{ GeV}^2$, which might then be taken as a rough estimate of the saturation scale for HERA data. However, one needs to be somewhat careful before jumping to the conclusion that the GBW dipole model shows that saturation effects have been seen at HERA. Given Eq. 9, $F_2 \sim 1/Q^2$ at low Q^2 is required in any model since the photoproduction cross-section is finite and slow, logarithmic scale breaking at high Q^2 is required by pQCD. Thus the real challenge is not in describing the general

⁵ As for example shown by the quark box at the top of Fig. 3.

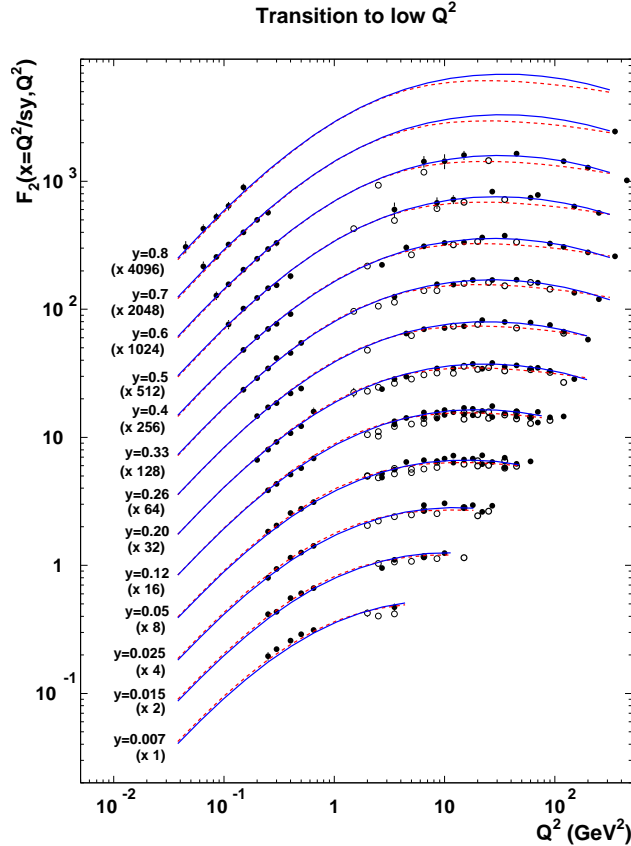


Fig. 10. The GBW dipole model fit to F_2 data through the transition region to photoproduction. The data are plotted versus Q^2 in bins of y . The dashed curves show the original model, the full curve the improved model with DGLAP evolution. From [16].

behaviour but in describing the exact shape of the data across the transition, now that high precision data are available. It should also be noted that there are other dipole models that fit the same data as successfully without an explicit x dependent saturation scale.

Although it gave a good description of F_2 at low Q^2 , the original GBW model did not include QCD evolution in Q^2 and this limited its success at larger Q^2 . This deficiency was corrected in a second version [16] in which $\hat{\sigma}$ was related to the gluon density. Results from both versions are shown in Fig. 10.

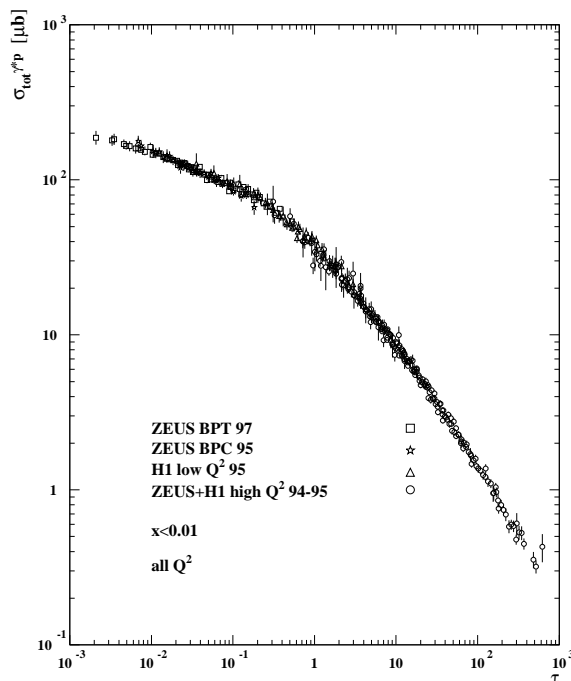


Fig. 11. Geometrical scaling. Data on $\sigma(\gamma^*p)$ with $x < 0.01$ plotted versus the scaling variable $\tau = Q^2 R_0^2(x)$. From [17].

Another feature of saturation models which is illustrated in the GBW model is the dependence of the dipole cross-section on a scaled variable, here $r/R_0(x)$. Stasto, Golec-Biernat and Kwiecinski [17] have made the interesting observation that this leads to a new scaling property of $\sigma(\gamma^*p)$. At low x , $\sigma(\gamma^*p)$ should depend only on the dimensionless variable $\tau = Q^2 R_0^2$. What is more, such a scaling property seems to be satisfied by HERA data. One expects

$$\sigma(\gamma^*p) \sim \sigma_0 \quad (\tau \text{ small}) \rightarrow \sigma(\gamma^*p) \sim \sigma_0/\tau \quad (\tau \text{ large}).$$

Fig. 11 shows HERA data with $x < 0.01$ as a function of τ . Not only do the data show this scaling very clearly, but also the expected change in behaviour indicated above seems to occur around values of $\tau \sim 1$. This new scaling – *geometrical scaling* – holds for Q^2 values up to about 400 GeV² but only for $x < 0.01$. Again, though it is not a proof, the remarkable demonstration of geometrical scaling by the low x HERA data does show that they have many of the attributes of a saturated system.

5. Summary

The low x data from HERA have produced many surprising and interesting results that can be understood in the perturbative dynamics of a gluon rich system, although details such as exactly how to include BFKL effects are as yet undecided. Whether saturation effects have been demonstrated at HERA is controversial, but whatever the answer to this question one cannot deny the importance of the measurements in stimulating activity in this area. Particularly encouraging are the attempts to describe high density gluon dynamics in terms of semi-classical models – the so-called ‘colour glass condensate’, which could be important for understanding data from heavy ion collisions at RHIC and the LHC.

Jan Kwiecinski has been active in most of these fields and his work can be seen as an attempt to understand and set scales on the map shown in Fig. 9. It has been a pleasure to profit from his insights and untiring efforts to unravel the dynamic structure of the proton.

REFERENCES

- [1] ZEUS Collab., Derrick M *et al.*, *Phys. Lett. B* **316** 412 (1993).
- [2] Askew A J *et al.* *Phys. Rev. D* **47** 3775 (1993).
- [3] Kwiecinski J, Martin A D, Roberts R & Stirling W J, *Phys. Rev. D* **42** 3645 (1990).
- [4] De Rujula A *et al.*, *Phys. Rev. D* **10** 1649 (1974).
- [5] Ball R D & Forte F, *Phys. Lett. B* **335** 77 (1994).
- [6] Glück M, Reya E & Vogt A, *Z. Phys. C* **48** 471 (1990).
- [7] ZEUS Collab., Chekanov S *et al.*, *Phys. Rev. D* **67** 0120071 (2003).
- [8] Kwiecinski J, Martin A D & Stasto A M, *Phys. Rev. D* **56** 3991 (1997).
- [9] Glück M, Reya E & Vogt A, *Z. Phys. C* **67** 433 (1995).
- [10] ZEUS Collab., Breitweg J *et al.*, *Eur. Phys. J. C* **7** 609 (1999).
- [11] Donnachie A & Landshoff P V, *Z. Phys. C* **61** 139 (1993).
- [12] Donnachie A & Landshoff P V (2001), *Phys. Lett. B* **518** 63 (2001).
- [13] Gayler J, [hep-ph/0211051], presented at the XXXII Int’l Symposium on Multiparticle Dynamics, Alushta, Crimea, Sept. 2002 and to be published in the proceedings, 2002.
- [14] Kwiecinski J, *J. Phys. G*. **19** 1443 (1993).
- [15] Golec-Biernat K & Wüsthoff M (1999), *Phys. Rev. D* **59** 014017 (1999), *Phys. Rev. D* **60** 114023 (1999).
- [16] Bartels J, Golec-Biernat K & Kowalski H, *Phys. Rev. D* **66** 014001 (2002).
- [17] Stasto A M, Golec-Biernat K & Kwiecinski J, *Phys. Rev. Lett.* **86** 596 (2001).